

## Supplementary Material for

Dossman BC, Rodewald AD, Studds CE, Marra PP. Migratory birds with delayed spring departure migrate faster but pay the costs. *Ecology*

### Appendix S1: Section S1 - Automated Telemetry & Motus Wildlife Tracking System

The local array in Jamaica consisted of 5 automated telemetry stations outfitted with a *Sensorgnome* receiver ([www.sensorgnome.org](http://www.sensorgnome.org)) and four horizontally polarized omnidirectional antennas positioned 9 meters high on a galvanized steel mast. One receiver was affixed with four 3-element directional Yagi antennas (oriented 90, 180, 270, and 0 degrees) and was situated on the northwest corner of the field site. The 3-element yagis provided better detection distances once birds were aloft and allowed for increased detection of birds and fine-scale assessment of individual trajectories upon departure.

The array located in northern Florida consisted of 6 *Sensorgnome* based automated telemetry towers, each affixed with at least two 9-element directional yagi's (PLC 1669, Laird Technologies) oriented East and West, respectively. The detection range of each tower was approximately 15 km (Mitchell et al. 2012, Taylor et al. 2017). By positioning these stations (approximately 30 km apart) across the narrowest point in Florida, we covered most of the migratory corridor used by our tagged birds.

Data collected by the automated telemetry system were uploaded to the Motus Wildlife Tracking System network for preliminary processing, archiving, and dissemination (Taylor et al. 2017). We used the R packages *Motus* (Brzustowski and LePage 2021) & *tidyverse* (Wickham et al. 2019) to download, filter, and analyze the data.

## Appendix S1: Section S2 - Light-level Geolocator Analyses

To identify the breeding origins of this population and to estimate the total time spent on migration, we equipped 45 (9-2017, 36-2019) individuals with a 0.32 g light-level geolocator (Intigeo-W30Z11-DIP, Migrate Technologies LTD., Cambridge, UK) using a modified leg-loop harness using stretch magic material. Of those deployed, four of 9 were recovered in 2018 and 11 of 36 were recovered in 2020 (19 of 36 returned but 11 recaptured) for a return rate of 51% which is significantly higher than the approximate 28% average geolocator return rate for similarly size warblers. Reported return rates in the literature include 35% Yellow Warbler (n=20)(Witynski and Bonter 2018), 47.5% Golden-winged Warbler (n = 40)(Peterson et al. 2015), 35.7% Kirtland's Warbler (n = 84)(Cooper et al. 2017), 27.5% Common Yellowthroat (n = 40) (Taff et al. 2018), 19% Canada Warbler (n = 154)(Roberto-Charron et al. 2020), 17% Cerulean Warbler (n = 28)(Delancey et al. 2020), and 14% Blackpoll Warbler (n=37)(DeLuca et al. 2015).

We followed methods outlined Lisovski et al. (2019) and the R package *GeolocTools* to analyze our light-level geolocator data. Data were downloaded, twilights were annotated using a threshold adjusted for each individual and manually annotated to conservatively mark outliers for exclusion in final analyses. Analysis of the movement tracks and stationary distributions were conducted in the *flightR* package (Rakhimberdiev et al. 2017). Calibrations were made with light-level data collected on tagged birds in the weeks prior to departure, which, for most birds, occurred after April 20<sup>th</sup>. Calibration periods ranged from 10 – 46 days. We set the spatial extent for our models to -90 – -120 degrees longitudinally and 18 – 55 degrees latitudinally. This extent conservatively captured our population's breeding and migratory distribution and improved computation efficiency for the particle filter. Particle filter runs were conducted with a million

particles. The breeding origins of these individuals were estimated by the hidden markov model implemented in the *flight package* and data can be found in *Supplementary Table S1*.

#### Appendix S1: Section S3 - Long-term Departure Survey Data

From 1994-2019, we followed a standardized protocol to monitor the spring departure schedules of, on average, 83 (range: 54 - 104) color-marked birds not outfitted with any other tag (Marra 1998). These surveys began on April 1<sup>st</sup> (before any documented migration occurs in this region) and continue through to May 15<sup>th</sup> by when the majority of the population has already departed. Color-banded individuals are resighted every three days that concludes with playback surveys if a bird was not detected sooner (see Marra (1998) and Studds & Marra (2011) for detailed description). The probability of resighting a color-banded individual is relatively high ( $p = 0.819$ , 95% CI: 0.807 – 0.831; Studds and Marra 2011) and comparable among habitats because redstarts actively defend small territories ( $0.16 \pm 0.5$  hectares) that are easy to survey (Marra et al. 2015). Therefore, individuals not detected within a three-day interval are assumed to have departed on the last night of the survey period. We excluded the rare cases where an individual abandoned a territory before April 15<sup>th</sup>, a week before the earliest migratory departures. In this manuscript, we only utilized the recent decade (2010-2019) to limit the effect that shifting departure schedules would have on our estimates of expected departure timing.

#### Appendix S1: Section S4 - Hierarchical Model Specification

$$\textbf{Sub Model 1: } Y_{ij} \sim \alpha_i + \beta_1 * Sex_i + \beta_2 * Rainfall_j + \beta_3 * Habitat_i + \beta_4 * d2H_i + \beta_5 * Rainfall_j * Habitat_i$$

$$\textbf{Sub Model 2: } Z_k \sim \gamma + \delta_1 * WindProfit_k + \delta_2 * RelativeMigratoryTiming_k$$

$$Expected\ Departure\ Date_k = \beta_1 * Sex_k + \beta_4 * d2H_k$$

$$\begin{aligned}
& \text{RelativeMigratoryTiming}_k \\
&= \text{Expected Departure Date}_k - \text{Observed Departure Date}_k \\
&\alpha_i \sim N(0,100), \quad \beta_i \sim N(0,100), \quad \delta_i \sim N(0,100)
\end{aligned}$$

#### Appendix S1: Section S5 - Stable Isotope Analysis

As a proxy for breeding latitude, we used the isotopic concentration of stable-hydrogen isotopes in tail feathers (3<sup>rd</sup> rectrix) known to be molted on the breeding grounds. Isotope analyses were conducted primarily at the Smithsonian Institution's Stable Isotope Mass Spectrometry Laboratory in Suitland, MD, USA. However, six samples were run at the Cornell Stable Isotope Lab (Ithaca, NY USA), following the exact sample protocols and standards. Efforts were made to standardize all procedures and materials used between laboratories.

Tail feathers were first rinsed in a 2:1 mixture of chloroform: methanol to remove surface oils and then subsequently allowed to equilibrate for 72h at the lab. Each feather's distal portion (length 3–5 mm) was sampled, weighed to  $350 \pm 10$  ug, and placed into a  $4 \times 6$ -mm silver capsule. Tissue samples were combusted in an elemental analyzer and introduced to an isotope ratio mass spectrometer via a ConFlo IV interface. One in-house standard was run for every 5 to 8 unknowns to measure accuracy and precision. The non-exchangeable hydrogen was determined by linear regression with calibrated in-house Keratin-based standards (Caribou Hoof Keratin, -196.90 ‰; Spectrum Keratin, -80.78 ‰; and Kudo Horn Keratin, -54.17 ‰). All stable hydrogen isotope ratios are in per mil units (‰).

#### Appendix S1: Section S6 - Assessing Wind Assistance

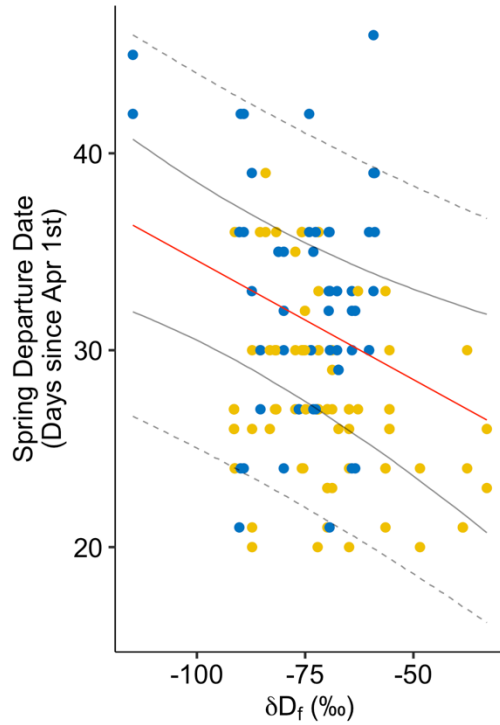
Wind assistance can influence the overall rate and survival during migration (Liechti and Schaller 1999, Drake et al. 2014, Clipp et al. 2020). We accounted for this confounding effect by first assessing how wind conditions varied across the departure window for this population of

redstarts (April 21 – May 12) and then included tailwind assistance in our migration rate model. For each individual, we calculated the mean daily tailwind component experienced while migrating between Jamaica and Florida using data from the NCEP-DOE Reanalysis 2. Averaged daily wind data presented in their easterly and northerly vector components (u & v, respectively) were acquired from the NCEP-DOE Reanalysis 2 (Kanamitsu et al. 2002) using the *RNCEP* package in R (Kemp et al. 2012) at a spatial resolution of 2.5° x 2.5° degrees. We used a simple vector model to estimate the tailwind assistance from the U and V components of wind velocity for a bird migrating at a bearing of 340° (towards Central Florida), which is the approximate average of bearings from individual tracks (range 336° - 344°). We constrained the spatial extent of our wind data to 20 - 27.5° N and 75 – 82.5°W corresponding to the region between Jamaica and Northern Florida—the likely airspace used by this population. Wind velocities are averaged across pressure-levels ranging from 1000 hPa (100 m.a.s.l) and 10 hPa (~26000 m.a.s.l). For simplicity and because wind conditions tend to be correlated at these lower altitudes (Gauthreaux et al. 2006) we used wind data from the 925 hPa pressure level (~760 m.a.s.l.), which is closer to the average for migratory passerines (< 1km m.a.s.l.) experiencing favorable wind conditions (e.g., tailwinds) at lower elevations (Dokter et al. 2011, Kemp et al. 2013).

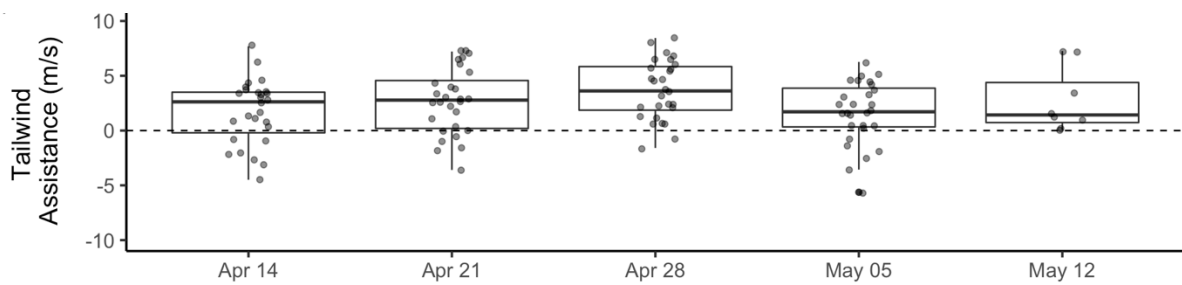
Appendix S1: Table S1 – Breeding origins of each individual American Redstart *Setophaga ruticilla* tagged with a light-level geolocator at Font Hill, Jamaica.

ID	SEX	AGE	BREEDING LATITUDE	BREEDING LONGITUDE	US STATE	WINTER DEPARTURE	BREEDING ARRIVAL	MIGRATION DURATION	MIGRATION DISTANCE	MIGRATION RATE
BQ700	SY	M	42.5240	-84.3119	MI	5/17/19	5/25/19	8	2780.34	14.48
BQ702	SY	M	42.4074	-91.5536	IA	5/2/19	5/23/19	21	2993.08	5.94
BQ703	SY	M	43.2482	-90.3429	WI	5/10/19	5/24/19	14	3028.85	9.01
BQ715	SY	M	42.7473	-90.1078	WI	5/7/19	5/30/19	23	2970.49	5.38
BQ716	SY	M	41.8808	-84.6511	MI	5/9/19	5/23/19	14	2718.60	8.09
BQ719	SY	M	40.6068	-88.2323	IL	5/15/19	5/23/19	8	2688.68	14.00
BQ731	SY	M	45.8373	-89.7670	WI	5/6/19	5/29/19	23	3270.40	5.92
BQ737	SY	M	43.8569	-92.5954	MN	5/7/19	5/30/19	23	3174.93	5.75
BQ738	SY	M	40.9496	-91.9245	IA	5/19/19	6/1/19	13	2869.77	9.20
BQ740	SY	M	43.8216	-90.5315	WI	5/18/19	6/2/19	15	3092.67	8.59
BQ741	SY	M	42.2079	-89.6525	IL	5/15/19	5/25/19	10	2900.19	12.08
BD622	ASY	M	43.6635	-92.5068	MN	4/27/17	5/26/17	29	3152.77	4.53
BD624	ASY	M	43.3294	-93.3125	IA	4/24/17	5/13/17	19	3154.75	6.92
BD626	ASY	M	41.7608	-92.3556	IA	4/27/17	6/9/17	43	2965.32	2.87
BD628	ASY	M	42.2885	-77.5770	NY	4/25/17	5/22/17	27	2688.19	4.15

Appendix S1: Figure S1 – American redstarts breeding at more northern latitudes depart relatively later in the season than individuals with southern breeding origins. Males departed an average of 4 days earlier than females (Figure S1;  $\beta_{\text{sex}} = -3.82$ , 95% CRI: - 5.98, - 1.60).

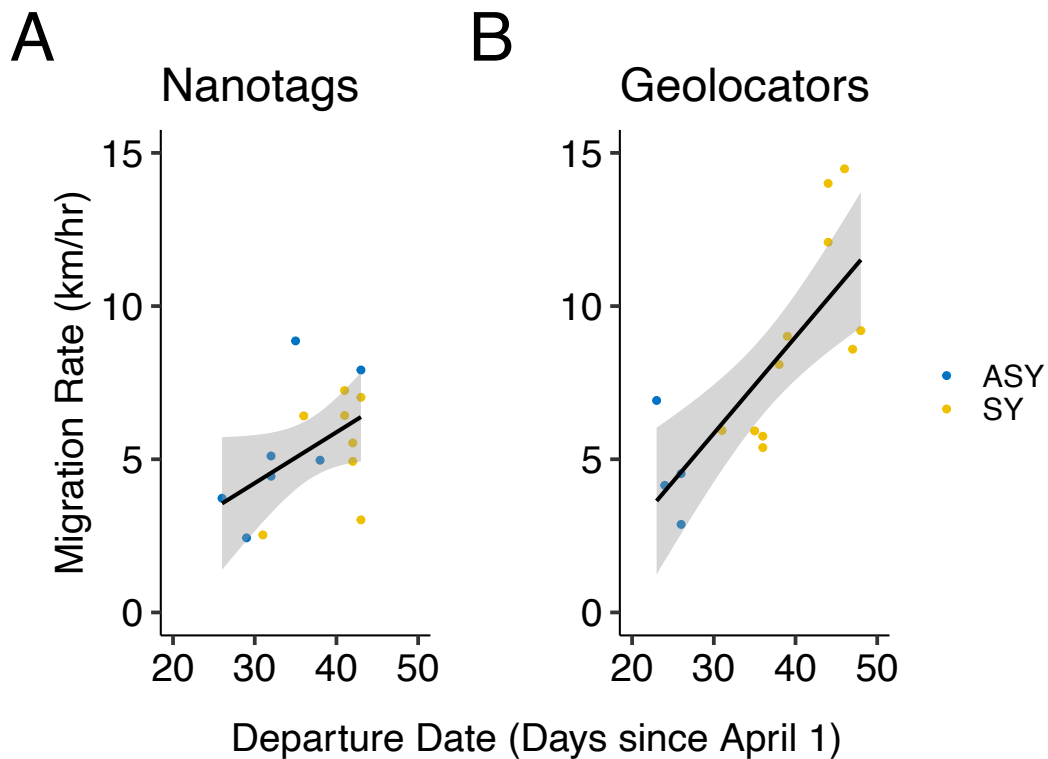


Appendix S1: Figure S2 – Predominant wind conditions during the migratory period for this wintering population (Apr 15 – May 15). In general winds were favorable for migration in the direction of travel and all birds, irrespective of departure week, experienced positive tailwind assistance.





Appendix S1: Figure S3 – Migration rates estimated via automated telemetry (A;  $5.37 \pm 1.95 \text{ km} \cdot \text{hr}^{-1}$ ) and light-level geolocators (B;  $7.79 \pm 3.5 \text{ km} \cdot \text{hr}^{-1}$ ). Migration rate estimated from an independent sample (N=15) of radio-tagged (nanotag) birds was found to be positive related to departure date (days since Apr 1). Similarly, migration rate estimated for a separate group (N=15) of individuals tagged with light-level geolocators was positively related to departure date (days since Apr 1).



- Brzustowski, J., and D. LePage. 2021. motus: Fetch and use data from the Motus Wildlife Tracking System. R package.
- Clipp, H. L., E. B. Cohen, J. A. Smolinsky, K. G. Horton, A. Farnsworth, and J. J. Buler. 2020. Broad-Scale Weather Patterns Encountered during Flight Influence Landbird Stopover Distributions. *Remote Sensing* 12:565.
- Cooper, N. W., M. T. Hallworth, and P. P. Marra. 2017. Light-level geolocation reveals wintering distribution, migration routes, and primary stopover locations of an endangered long-distance migratory songbird. *Journal of Avian Biology* 48:209–219.
- Delancey, C. D., K. Islam, G. R. Kramer, G. J. MacDonald, A. R. Sharp, and B. M. Connare. 2020. Geolocators reveal migration routes, stopover sites, and nonbreeding dispersion in a population of Cerulean Warblers. *Animal Migration* 7:19–26.
- DeLuca, W. V., B. K. Woodworth, C. C. Rimmer, P. P. Marra, P. D. Taylor, K. P. McFarland, S. A. Mackenzie, and D. R. Norris. 2015. Transoceanic migration by a 12 g songbird. *Biology Letters* 11:20141045.
- Dokter, A. M., F. Liechti, H. Stark, L. Delobbe, P. Tabary, and I. Holleman. 2011. Bird migration flight altitudes studied by a network of operational weather radars. *Journal of the Royal Society Interface* 8:30–43.
- Drake, A., C. A. Rock, S. P. Quinlan, M. Martin, and D. J. Green. 2014. Wind Speed during Migration Influences the Survival, Timing of Breeding, and Productivity of a Neotropical Migrant, *Setophaga petechia*. *PLoS ONE* 9:e97152.
- Gauthreaux, S. A., C. G. Belser, and C. M. Welch. 2006. Atmospheric trajectories and spring bird migration across the Gulf of Mexico. *Journal of Ornithology* 147:317–325.
- Kanamitsu, M., W. Ebisuzaki, J. Woollen, S.-K. Yang, J. J. Hnilo, M. Fiorino, and G. L. Potter. 2002. NCEP–DOE AMIP-II Reanalysis (R-2). *Bulletin of the American Meteorological Society* 83:1631–1643.
- Kemp, M. U., E. E. van Loon, J. Shamoun-Baranes, and W. Bouten. 2012. RNCEP: global weather and climate data at your fingertips. *Methods in Ecology and Evolution* 3:65–70.
- Kemp, M. U., J. Shamoun-Baranes, A. M. Dokter, E. Loon, and W. Bouten. 2013. The influence of weather on the flight altitude of nocturnal migrants in mid-latitudes. *Ibis* 155:734–749.

- Liechti, F., and E. Schaller. 1999. The Use of Low-Level Jets by Migrating Birds. *Naturwissenschaften* 86:549–551.
- Marra, P. P., C. E. Studds, S. Wilson, T. S. Sillett, T. W. Sherry, and R. T. Holmes. 2015. Non-breeding season habitat quality mediates the strength of density-dependence for a migratory bird. *Proceedings of the Royal Society B: Biological Sciences* 282:20150624.
- Mitchell, G. W., A. E. M. Newman, M. Wikelski, and D. R. Norris. 2012. Timing of breeding carries over to influence migratory departure in a songbird: an automated radiotracking study. *Journal of Animal Ecology* 81:1024–1033.
- Peterson, S. M., H. M. Streby, G. R. Kramer, J. A. Lehman, D. A. Buehler, and D. E. Andersen. 2015. Geolocators on Golden-winged Warblers do not affect migratory ecology. *The Condor* 117:256–261.
- Roberto-Charron, A., J. Kennedy, L. Reitsma, J. A. Tremblay, R. Krikun, K. A. Hobson, J. Ibarzabal, and K. C. Fraser. 2020. Widely distributed breeding populations of Canada warbler (*Cardellina canadensis*) converge on migration through Central America. *BMC Zoology* 5:10.
- Taff, C. C., C. R. Freeman-Gallant, H. M. Streby, and G. R. Kramer. 2018. Geolocator deployment reduces return rate, alters selection, and impacts demography in a small songbird. *PLoS ONE* 13:e0207783.
- Taylor, P., T. Crewe, S. Mackenzie, D. Lepage, Y. Aubry, Z. Crysler, G. Finney, C. Francis, C. Guglielmo, D. Hamilton, R. Holberton, P. Loring, G. Mitchell, D. R. Norris, J. Paquet, R. Ronconi, J. Smetzer, P. Smith, L. Welch, and B. Woodworth. 2017. The Motus Wildlife Tracking System: a collaborative research network to enhance the understanding of wildlife movement. *Avian Conservation and Ecology* 12.
- Wickham, H., M. Averick, J. Bryan, W. Chang, L. McGowan, R. François, G. Grolemund, A. Hayes, L. Henry, J. Hester, M. Kuhn, T. Pedersen, E. Miller, S. Bache, K. Müller, J. Ooms, D. Robinson, D. Seidel, V. Spinu, K. Takahashi, D. Vaughan, C. Wilke, K. Woo, and H. Yutani. 2019. Welcome to the Tidyverse. *Journal of Open Source Software* 4:1686.
- Witynski, M. L., and D. N. Bonter. 2018. Crosswise migration by Yellow Warblers, Nearctic-Neotropical passerine migrants. *Journal of Field Ornithology* 89:37–46.